

## Cellular and tissue expression of DAPIT, a phylogenetically conserved peptide

H. Kontro,<sup>1,2</sup> J.J. Hulmi,<sup>3</sup> P. Rakkila,<sup>4</sup> H. Kainulainen<sup>3</sup>

<sup>1</sup>Institute of Biomedical Technology, University of Tampere

<sup>2</sup>Pediatric Research Center, University of Tampere;

<sup>3</sup>Department of Biology of Physical Activity, University of Jyväskylä;

<sup>4</sup>Department of Health Sciences, University of Jyväskylä, Finland

### Abstract

DAPIT (Diabetes Associated Protein in Insulin-sensitive Tissues) is a small, phylogenetically conserved, 58 amino acid peptide that was previously shown to be down-regulated at mRNA level in insulin-sensitive tissues of type 1 diabetes rats. In this study we characterize a custom made antibody against DAPIT and confirm the mitochondrial presence of DAPIT on cellular level. We also show that DAPIT is localized in lysosomes of HUVEC and HEK 293T cells. In addition, we describe the histological expression of DAPIT in several tissues of rat and man and show that it is highly expressed especially in cells with high aerobic metabolism and epithelial cells related to active transport of nutrients and ions. We propose that DAPIT, in addition to indicated subunit of mitochondrial F-ATPase, is also a subunit of lysosomal V-ATPase suggesting that it is a common component in different proton pumps.

### Introduction

DAPIT is a 58 amino acid peptide, which was previously discovered in insulin-sensitive tissues of rats that were rendered diabetic by streptozotocin.<sup>1</sup> Afterwards, it was shown that it is a component of mitochondrial ATP synthase<sup>2,3</sup> (also called F-ATPase) and regulates ATP synthase population in mitochondria.<sup>4</sup> DAPIT is the protein product of *Usmg5* (also called *Dapit*) gene that is conserved from insects to vertebrates. It contains a single presumed  $\alpha$ -helix spanning from amino acid 23 to 45. The predicted length of the  $\alpha$ -helix varies marginally (1-3 amino acids), depending on the software used. In addition, DAPIT has a poor but recognizable similarity with a putative yeast ortholog.<sup>3</sup> This similarity over the species depicts the conceivable importance

and conserved function of DAPIT. The chromosomal location of *Usmg5* gene is 1q54 in rat, 19D1 in mouse and 10q24 in man.

Since proteomics approach has identified DAPIT as a subunit of F-ATPase,<sup>2,3</sup> we wanted to confirm this result on cellular level in human and rodent cells. F-ATPase and vacuolar-ATPase (V-ATPase) are related to each other structurally and mechanistically wise,<sup>5,6</sup> therefore, we also studied the DAPIT involvement with V-ATPase by immunofluorescence. We previously investigated the mRNA expression of DAPIT in insulin-sensitive tissues of normal and streptozotocin diabetic rats;<sup>1</sup> in the present study we investigated the DAPIT protein expression in this type 1 diabetic model and show its histological expression in several normal rat and human tissues. Based on the results of all these studies, we confirm the mitochondrial location of DAPIT and show its new localization in lysosomes containing V-ATPase. In addition, we describe DAPIT expression in the insulin-sensitive tissues of diabetic rat and mouse, and its histological expression in several rat and human tissues.

### Materials and Methods

#### DAPIT antibody

For the detection of DAPIT, polyclonal IgG antibodies  $\alpha$ D15N and  $\alpha$ D15C against the amino- and carboxyterminal peptides (MAGPESDGGQFQTGI and YFKLRPKKTPAVKAT, respectively) of rat DAPIT were raised in rabbits (Davids Biotechnologie, Regensburg, Germany). The animals were immunized once intra-dermally followed by four intra-muscular immunizations. The sera were collected for the affinity purification of IgG. The concentrations of affinity purified IgG fractions were determined by ELISA being 0.38 mg/mL for  $\alpha$ D15N and 0.16 mg/mL for  $\alpha$ D15C. All the experiments utilizing these antibodies were repeated three times, except the Western blot of rat and mouse tissues. This was repeated twice with two pairs of control and diabetic rats and 2-3 times with mouse samples.

#### Animals and human samples

The control and streptozotocin diabetic rats were described previously.<sup>1</sup> Diabetes was confirmed by serum glucose that was >600 mg/dL 7 days after the injection of streptozotocin (STZ). The control and STZ-mice were reported in detail elsewhere.<sup>7</sup> Human tissue samples were collected during resection of carcinomas. Healthy appearing pieces of the liver adenocarcinoma sample of a 48-year-old female and kidney clear cell carcinoma of a 68-year-old male were used for immunohistochemistry.

Correspondence: Prof. Heikki Kainulainen, Department of Biology of Physical Activity, University of Jyväskylä, PO Box 35, FIN-40014. Tel. +358.50.3302901 – Fax: +358.14.2602071. E-mail: Heikki.Kainulainen@sport.jyu.fi

Key words: DAPIT, mitochondrion, V-ATPase, type 1 diabetes.

Acknowledgments: this work was supported by the *Competitive Research Funding* of the Pirkanmaa Hospital District, the *Diabetes Research Foundation*, the *Finnish Cultural Foundation*, *Pirkanmaa Regional fund*, and the *Academy of Finland*. The authors would like to thank Eric Dufour for his critical view of the manuscript and Marja-Leena Koskinen for her skillful technical assistance.

Contributions: HKa, HKo, study design, coordination, cell and rat experiments planning and carrying out, manuscript drafting; JJH, mouse protein studies carrying out; PR, mouse microscopy. All authors read and approved the final manuscript.

Conflict of interests: the authors declare no conflict of interests.

Received for publication: 12 December 2011.

Accepted for publication: 13 March 2012.

This work is licensed under a Creative Commons Attribution NonCommercial 3.0 License (CC BY-NC 3.0).

©Copyright H. Kontro et al., 2012

Licensee PAGEPress, Italy

European Journal of Histochemistry 2012; 56:e18

doi:10.4081/ejh.2012.e18

#### Cell lines and cell culture

Human embryonic kidney-derived HEK 293T cells were a kind gift from the laboratory of Howard T. Jacobs, Institute of Biomedical Technology, Tampere, Finland. The cells were cultured in Dulbecco's modified Eagle medium (Sigma-Aldrich, Ayshire, UK, or Gibco brl, Paisley, Scotland, UK), containing 4.5 g/L of D-glucose, 10% foetal calf serum (Sigma), 50  $\mu$ g/mL uridine, 1 mM sodium pyruvate, 2 mM L-glutamine, and 100 U penicillin and 100  $\mu$ g/mL of streptomycin (Gibco) at 37°C in an incubator with 5% CO<sub>2</sub> in air. Mouse myoblasts (C2C12) were a kind gift from Antero Salminen, University of Kuopio, Finland. These cells were maintained in Dulbecco's modified Eagle's medium (DMEM/F12, Gibco) containing 4.5 g/L D-glucose, 10% foetal calf serum, 0.075% sodium bicarbonate (Gibco), and 100 U penicillin and 100  $\mu$ g/mL streptomycin. Cells were passaged routinely every 3-4 days at 1:10 and 1:4 dilution. HEK 293T cells were detached by pipetting and C2C12 by treat-

ment with Trypsin-EDTA (Gibco). Human Umbilical Vein Endothelial Cells (HUVEC) were purchased from Lonza (Cambrex Bio Science, Walkersville, MD, USA), maintained in HuMedia-EGM™ (EGM-1) (Clonetics®, San Diego, CA, USA) and subdivided 1:6 when confluent. In all experiments performed, the cells were used between passages 2 and 6.

All cells were seeded on cover slips or in culture slides (BD Biosciences, Erembodegem, Belgium) one to three day prior to use. The glassware was coated with 20% poly-L-lysine (Sigma) when needed.

### Fluorescence microscopy

For the staining of mitochondria and lysosomes, the cells were washed with PBS and incubated in a medium containing 100 nM Mitotracker Red or LysoTracker Red (Invitrogen Molecular Probes, Leiden, The Netherlands) for 10-30 min at 37°C. After washing, normal medium was added to the Mitotracker stained cells and incubated for further 30-60 min at 37°C. For transient translation of amino- and carboxyterminal fusion proteins of DAPIT and GFP in HEK 293T cells, DAPIT was cloned into pEGFP-N3 and pEGFP-C1 vectors (Clontech Laboratories, Palo Alto, CA, USA). In immunofluorescence, the Tris Buffered Saline-Tween (TBS-T) (10 mM Tris, 0.9% NaCl, pH 8.0, 0.1% Tween 20, Sigma) was used. The cells were fixed at room temperature with 4% paraformaldehyde (Sigma) for 15 min, permeabilized with 0.5% Triton X-100 (Sigma) for 10 min and blocked with 5% w/v non-fat milk powder and 2% BSA (Sigma) for 30 min. The cells were single- or double-stained with the rabbit polyclonal antibody against DAPIT (reported above,  $\alpha$ D15N 1:800,  $\alpha$ D15C 1:320 and antibodies preincubated overnight at 4°C with 4x excess of peptide of issue) and goat

polyclonal antibody against V-ATPase subunit H (SC-21228, Santa Cruz, CA, USA, 1:800) for 2 h. After intensive washing with TBS-T the primary antibodies were detected by donkey anti-

rabbit IgG conjugated with Alexa Fluor 488 (Invitrogen, 1:4000) and donkey anti-goat IgG conjugated with Alexa Fluor 555 (Invitrogen, 1:4000) for 1 h. After washes the coverslips

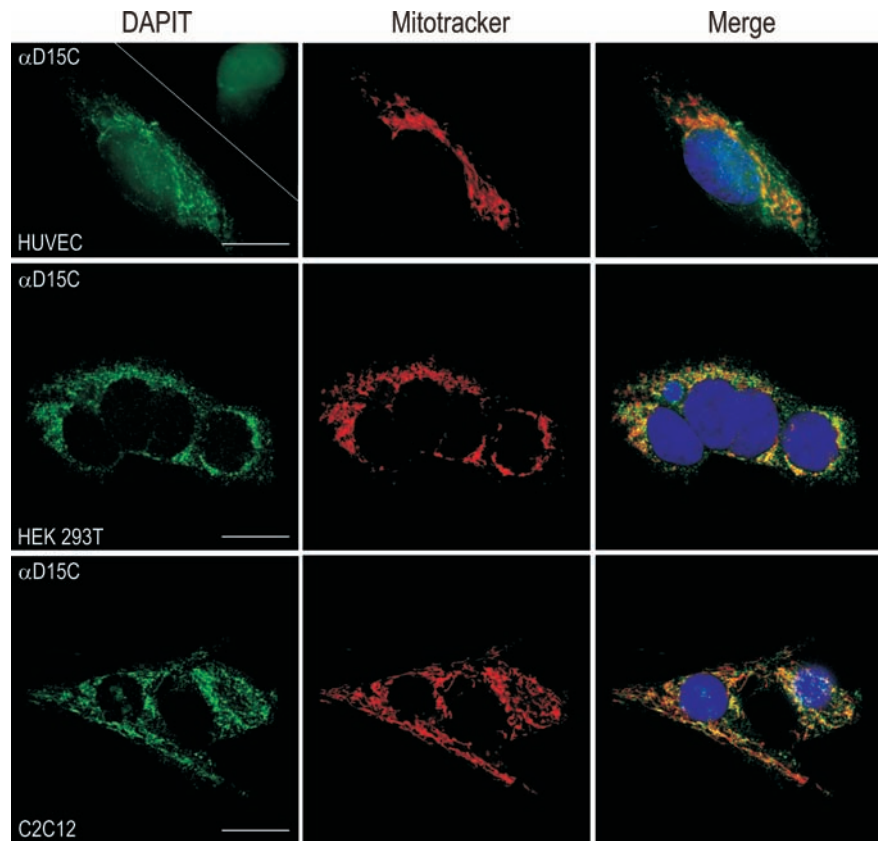


**Figure 1.** DAPIT locates into mitochondria in HUVEC, HEK 293T and C2C12 cells. In the upper right corner of the green picture in HUVEC is shown the staining with peptide-blocked C-terminal antibody. The pictures of HUVEC cells were taken by traditional fluorescence microscope, and the ones of HEK 293T and C2C12 cells by confocal microscope. Nuclei-staining with DAPI. Scale bars 25  $\mu$ m.

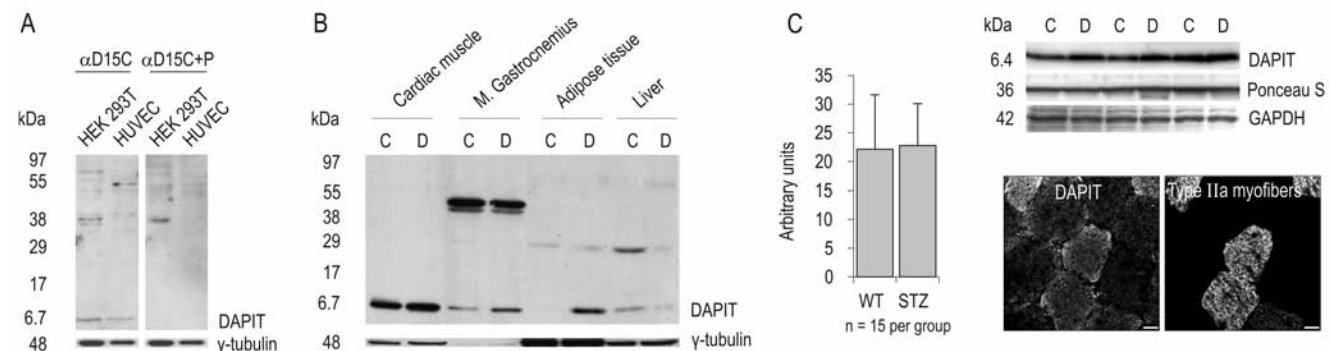


**Figure 2.** DAPIT expression in protein level. SDS-PAGE with: A) antibody and peptide-blocked antibody against DAPIT; B) healthy and early stage diabetic insulin-sensitive tissues of rat; C) DAPIT in healthy and STZ-induced diabetic insulin-sensitive calf muscle complex of mice (C, control; D, diabetic). Cross-section of mouse skeletal muscle shows more DAPIT in type IIa (highly oxidative) myofibers, which contain more mitochondria, than other myofibers. Scale bars: 20  $\mu$ m.

were mounted on slides using Vectashield mounting medium (Vector Laboratories, Burlingame, CA, USA). All samples were examined at 100x magnification by confocal microscopy, using a Perkin Elmer-Cetus/Wallac UltraView LCI system (Wellesly, MA, USA) equipped with appropriate excitation and emission filters and an Andor iXon DV885 EMCCD camera and the Andor iQ software (Andor, Belfast, UK), or a traditional fluorescence microscope, ColorView III camera and the Cell imaging software (Olympus BX60, Olympus Corp., Tokyo, Japan). Images were further processed using Corel Photo-Paint 11 (Corel Corp., Ottawa, ON, Canada).

Ten micrometer thick cryosections from mouse *gastrocnemius* muscle were fixed with 4% PFA for 15 min, permeabilized with 0.5% Triton-X100 for 10 min and blocked with 3% BSA for 1 h. Sections were double-stained with a mouse monoclonal antibody against fast myosin type II a developed by Dr. H.M Blau<sup>8</sup> (SC-71, Developmental Studies Hybridoma Bank, University of Iowa, Iowa City, USA, 1:50) to detect most oxidative fibers and C-terminal rabbit polyclonal DAPI antibody (*see above*) for 1 h at room temperature. After intensive washing with PBS the primary antibodies were detected by a mixture of goat anti-mouse antibody conjugated with Alexafluor 488 (Invitrogen, 1:400) and the polyclonal antibody with goat anti-rabbit antibody conjugated with Alexafluor 546 (Invitrogen, 1:400) for 1 h. After washing with PBS the sections were mounted with Mowiol (Sigma) including 2.5% DABCO (Sigma). The samples were viewed with Olympus BX 51 epifluorescence microscope. Images were captured by ColorView III camera and Analysis Five software (Olympus Corp.).

### Immunohistochemistry

Sections of paraffin-embedded tissues from the rat myocardium, skeletal muscle, adipose tissue, liver, kidney, brain and small bowel, and human liver and kidney were used for immunohistochemical staining applying the standard immunoperoxidase method. Briefly, 4  $\mu$ m thick paraffin sections were cut and deparaffinized. The antigen retrieval of the sections was performed by boiling in a microwave oven for 15 min in 0.01 M citrate buffer (pH 6.0) followed by cooling to room temperature. After washing in PBS, non-specific binding sites were blocked by incubating the sections in normal goat serum for 1 h. Subsequently, the sections were incubated overnight at 4°C with  $\alpha$ D15C antibody (dilution 1:150-1:200) followed by an incubation in the secondary antibody (biotinylated anti-rabbit IgG, Vector Laboratories, 1:100) for 30 min. Endogenous peroxidase activity was removed using 0.3%

H<sub>2</sub>O<sub>2</sub> for 30 min. ABC-reaction was done with the Vectabond TM reagent (Vector Laboratories) for 30 min at room temperature. Antigen-antibody complexes were visualized using diaminobenzidine (DAB DacoCytomation Inc., Carpinteria, CA, USA) as the chromogen. Finally, the sections were counterstained with Mayer's hematoxylin (Merck KGaA, Darmstadt, Germany), washed with tap water, dehydrated and mounted with Pertex mounting medium. Sections incubated with the peptide-blocked antibody or without the primary antibody served as negative controls.

### Western blot analysis

The expression level of DAPIT was studied by Western blot in HEK 293T and HUVEC cells, in healthy and diabetic rat myocardium and *m. gastrocnemius*, epididymal adipose tissue and liver, and also in mouse calf muscle complex (*gastrocnemius*, *soleus*, *plantaris*). The tissue samples were incubated or homogenized in 0.5 ml of buffer containing (1% Triton X100 in standard PBS, protease inhibitor mixture (Roche Applied Science, Rotkreuz, Switzerland) and 3 mM phenylmethylsulfonyl fluoride (PSMF) (Calbiochem/Merck) followed by an incubation on ice for 30 min and centrifugation at 12,000 g for 1 min. The cells from confluent 100x20mm cell culture dishes were treated in a similar way without homogeniza-

tion.

The protein concentration was determined by Bradford method. Twenty  $\mu$ g (rat and cellular) and 30  $\mu$ g (mouse) of protein, was heated at 95 °C for 5 min in SDS-PAGE sample buffer<sup>9</sup> prior to loading on the gel, run on 12% acrylamide SDS-PAGE according to standard protocol<sup>10</sup> and blotted electrophoretically at 100 V for 1 h at 4°C to Hybond-C extra nitrocellulose membrane (Amersham Int. plc, Buckinghamshire, UK). Blots were blocked with TBS-T containing 5% freeze-dried fat-free milk powder for 1 h and incubated with primary antibody ( $\alpha$ D15C 1:160 and peptide blocked antibody, mouse monoclonal antibody against  $\gamma$ -tubulin (T5326, Sigma) 1:4000, ATP synthase subunit alpha monoclonal antibody produced in mouse (MS502, Abcam, Eugene, OR, USA) 1:4000 and goat polyclonal IgG against cytochrome C (Sc-8385, Santa Cruz, CA, USA) 1:1000) for 2 h. After washings, the blots were incubated in the secondary antibody (peroxidase-conjugated swine anti-rabbit and rabbit anti-mouse (DAKO, Clostrup, Denmark) 1:2000, and Peroxidase Horse Anti-Goat IgG (H+L) (Vector Laboratories, 1:10000) for 1 h. Subsequently, the blots were washed and the signal was detected by enhanced chemiluminescent ECL<sup>TM</sup> reagent (Amersham Int.) according to the manufacturer's protocol. The blots were visualized on Super RX medical X-

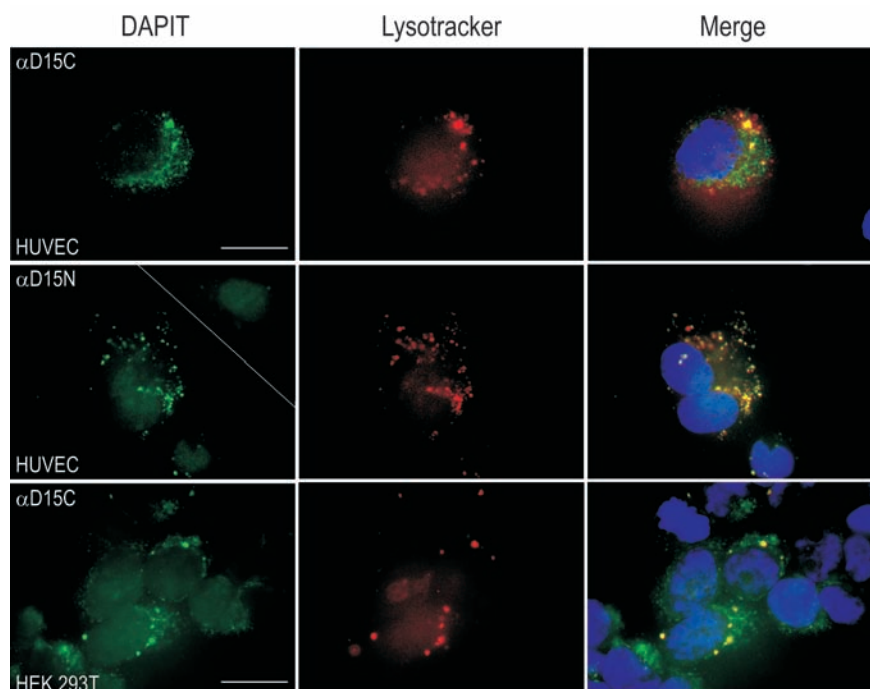


**Figure 3.** DAPI locates into lysosomes in HUVEC, HEK 293T and C2C12 cells. In the upper right corner of the green picture in the middle row is shown the staining with peptide-blocked N-terminal antibody. Nuclei-staining with DAPI. Scale bars: 25  $\mu$ m.



ray film (Fujifilm Corp., Tokyo, Japan) using 3–20 min exposure times.

## Ethical permissions

Animal experiments were approved by the Animal Experimentation Committee of the University of Tampere and Jyväskylä. The Ethical Committee of Tampere University Hospital approved the use of human tissues.

## Results

### Specificity of $\alpha$ D15N and $\alpha$ D15C antibodies

We used a custom made  $\alpha$ D15N and  $\alpha$ D15C polyclonal antibody against amino- and carboxyterminus of DAPIT, a small, phylogenetically conserved protein. In transient transfection studies in HEK 293T cells,  $\alpha$ D15C colocalized with DAPIT fused to the C-terminus of GFP and, respectively,  $\alpha$ D15N recognized DAPIT fused to the N-terminus of GFP (*results not shown*).

We further studied the specificity of  $\alpha$ D15C antibody by immunofluorescence microscopy in human HUVEC endothelial and HEK 293T kidney cells, and mouse C2C12 myocytes. Incubation of the cell samples with the antigen-blocked antibody abolished all DAPIT staining as shown in left upper panel in Figure 1. The cross-over reactions between anti-rabbit and anti-goat IgG secondary antibodies with the non-corresponding primary antibody were negative. The approximately 6.7 kDa band corresponding to the calculated molecular weight of DAPIT (6.407 kD) disappeared also in SDS-PAGE upon peptide blocking of the antibody (Figure 2A). The  $\alpha$ D15N antibody was specific in HUVEC-cells by immunofluorescence (Figure 3, middle panel). The specificity of the C-terminal antibody was also studied by Western blot in rat cardiac and skeletal muscle (Figure 2B). The antibody recognized DAPIT in both muscle types. In skeletal muscle also a protein of ca 50 kDa was seen. All bands disappeared upon peptide blocking of the antibody. In mouse this size of protein was not detected.

Also DAPIT staining in histological samples was negative after the omission of secondary antibody and peptide-blocking of the  $\alpha$ D15C confirming further the specificity of the  $\alpha$ D15C antibody (Figure 4).

### Cellular localization of DAPIT

We confirmed DAPIT localization to mitochondria by immunofluorescence in human and rodent cell lines. DAPIT colocalized with Mitotracker (*i.e.* mitochondria) in HUVEC, HEK 293T and C2C12 cells (Figure 1). Due to

the reported similarity of the structure of F-ATPase and V-ATPase, we studied DAPIT localization in vacuoles like lysosomes, which are known to contain a lot of hydrogen pumps. Our amino- and carboxyterminal antibodies against DAPIT colocalized with Lysotracker (Figure 3) and V-ATPase (Figure 5) in HUVEC and HEK 293T cells. The N-terminal antibody against DAPIT did not recognize the mitochondrial form of the protein in HUVEC cells, whereas in HEK 293T cells the antibody did not recognize any specific structures (*results not shown*). The vacuolar expression of DAPIT was more abundant in HUVEC than in HEK 293T cells. The lysosomal localization of DAPIT in both cell lines was also detected with N- and C-

terminal GFP-fusionproteins and with Lysotracker and antibodies against LAMP 24 h after transient transfections (*results not shown*).

### Tissue expression of DAPIT

The expression of DAPIT was investigated in several healthy rat and human tissues by immunohistochemistry (Figure 4). The antibody against carboxyterminal end of the protein was used. The expression of DAPIT varied in intensity within a tissue and from one tissue to another, showing mainly cytoplasmic staining and also occasional staining in some nuclei. The expression in cytoplasm varied exhibiting both smeary and finely granular

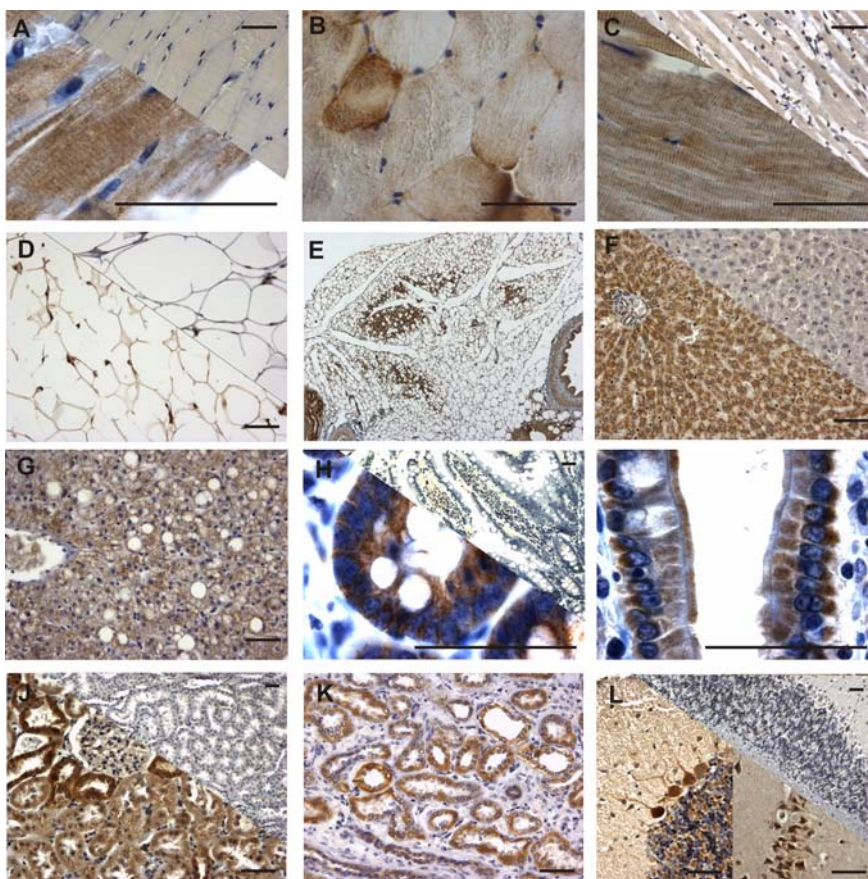


**Figure 4.** Immunohistochemical staining of DAPIT with  $\alpha$ D15C antibody in rat and human tissues. Negative control stainings were performed using antigen-blocked antibody or by omitting the primary antibody (upper right corner of A, C, D, F, H, J and L). A,B) Myofibers of rat skeletal muscle; longitudinal section (A) shows sarcomere-like staining; in crosssections (B) differential staining of fibers is notable. C) In rat myocardium sarcomere-like staining was also seen. D,E) Adipocytes of rat epididymal adipose tissue (D) and adipose tissue surrounding kidney showed cytoplasmic staining; islands of brown adipose tissue (E) seen within the white adipose tissue were strongly stained. F) Rat and G) human hepatocytes showed granular cytoplasmic staining that was more intense in hepatocytes surrounding veins and bile ducts. H) Crypt and I) villus epithelial cells of the rat small intestine exhibited cytoplasmic and also some nuclear staining. In the villi the staining was seen specifically both in basal and apical sides of the nuclei. J) In the rat and K) human kidneys variable staining was seen in the epithelial cells of convoluted proximal tubules. L) In the rat, especially Purkinje cells of the cerebellum (left) and pyramidal neurons in the hippocampus were strongly stained. Scale bars: 50  $\mu$ m.

staining patterns.

In general, the strongest DAPIT expression was observed in insulin-sensitive and epithelial cells as well as in neurons. Cardiocytes and myofibers showed strong expression of DAPIT complying the sarcomeric structure (Figure 4A-C). Skeletal muscle cells showed considerable differences in their staining intensities. Double staining with type IIa-specific myosin antibody demonstrated that DAPIT was more abundant in highly oxidative (type IIa) than in less oxidative or glycolytic muscle fibers and located preferentially under the sarcolemma (Figure 2C). Adipocytes of white and brown adipose tissue (Figure 4D,E) showed distinct cytoplasmic staining that was considerably stronger in brown fat. In hepatocytes, granular cytoplasmic staining was observed (Figure 4F,G). This staining and granularity tended to be more intensive in the cells surrounding blood vessels and bile ducts. Epithelial cells of rat small intestine were stained from the base of the crypt to the villus tips showing also some nuclear staining (Figure 4H,I). The epithelial cells of proximal tubuli in kidney were intensively stained (Figure 4J,K) showing, however, considerable difference in staining intensity from cell to cell. Purkinje cells of cerebellum and pyramidal cells of hippocampus were

strongly stained in rat brain (Figure 4L). The stainings with the antibody against aminoterminal end of DAPIT were similar to those of the carboxyterminal antibody (*results not shown*).

Previously, we showed that DAPIT mRNA is down-regulated in the rat skeletal muscle and myocardium in streptozotocin-induced diabetes.<sup>1</sup> Here we studied first qualitatively the level of protein expression of DAPIT in insulin-sensitive tissues of two pairs of control and diabetic rats. We found that DAPIT was up-regulated in the diabetic myocardium, m. gastrocnemius and epididymal adipose tissue but down-regulated in the liver in the early stage of diabetes in rat (Figure 2B). We also found up-regulated DAPIT expression in diabetic *m. soleus* and down-regulation in *m. plantaris* (*results not shown*). Western blot showed also two tissue specific bands of ~50 kDa in skeletal muscle but not in the other tissues.

In contrast to rats, no changes in quantified expression of DAPIT was seen in comparing healthy and diabetic calf muscle complexes (gastrocnemius, soleus, plantaris) of mice with diabetes for 1-5 weeks (Figure 2C). Notably, however, DAPIT correlated well with the mitochondrial proteins cytochrome c ( $r=0.450$ ,  $P=0.014$ ) and ATP synthase subunit

alpha ( $r=0.689$ ,  $P\leq 0.001$ ) in mouse skeletal muscle.

## Discussion

DAPIT is 58 amino acid peptide with single transmembrane helical span that in mRNA level is down-regulated in insulin-sensitive tissues in streptozotocin-induced diabetes.<sup>1</sup> In this study we show by peptide-blocking that our custom made antibody against aminoterminal end of DAPIT recognizes the vacuolar structures in immunofluorescence in HUVEC. The carboxyterminal antibody against DAPIT is specific in Western blot, immunofluorescence and immunohistochemistry. It recognizes the right size of the protein, the reported mitochondrial location of the protein, and also previously unreported vacuolar structures. However, in skeletal muscle of rat but not mouse, the carboxyterminal DAPIT antibody detected also a ~50 kDa protein. At the moment, protein databases do not recognize any proteins of greater size than DAPIT with the antigenic sequence used to raise the specific antibody. It remains to be shown if a still unknown longer isoform of DAPIT or an unknown skeletal muscle-specific protein exists. Therefore, it cannot be ruled out that the antibody detects also another protein in skeletal muscle in immunohistochemistry.

Previously, DAPIT was shown to associate with the ATP synthase from bovine heart mitochondria<sup>2,3</sup> and suggested to contribute to the formation of this enzyme.<sup>2</sup> In the present study we confirmed the mitochondrial location of DAPIT in three different cell lines by immunofluorescence microscopy using the specific polyclonal antibody that was raised against the carboxy terminus of DAPIT. Significant correlations of DAPIT with cytochrome c and ATP synthase subunit alpha further supported the observed close association of DAPIT with mitochondria.

In addition, we could detect DAPIT also in other structures than mitochondria that prompted us to study its possible colocalization with other organelles. DAPIT colocalized abundantly with acidic organelles labelled by LysoTracker and antibody against V-ATPase in HUVEC and HEK 293T cells. Vacuolar ATPases are structurally and mechanistically related to mitochondrial F-ATPase.<sup>5,6</sup> Both F-ATPase and V-ATPase consist of a membrane domain  $V_0$  and a catalytic domain  $V_1$ , and operate *via* rotary mechanism.<sup>11</sup> V-ATPases are ATP-driven proton pumps that acidify intracellular compartments and transport protons across the plasma membrane. V-ATPases have been identified *e.g.* in lysosomes, secretory vesicles and plasma membrane, and they are involved in

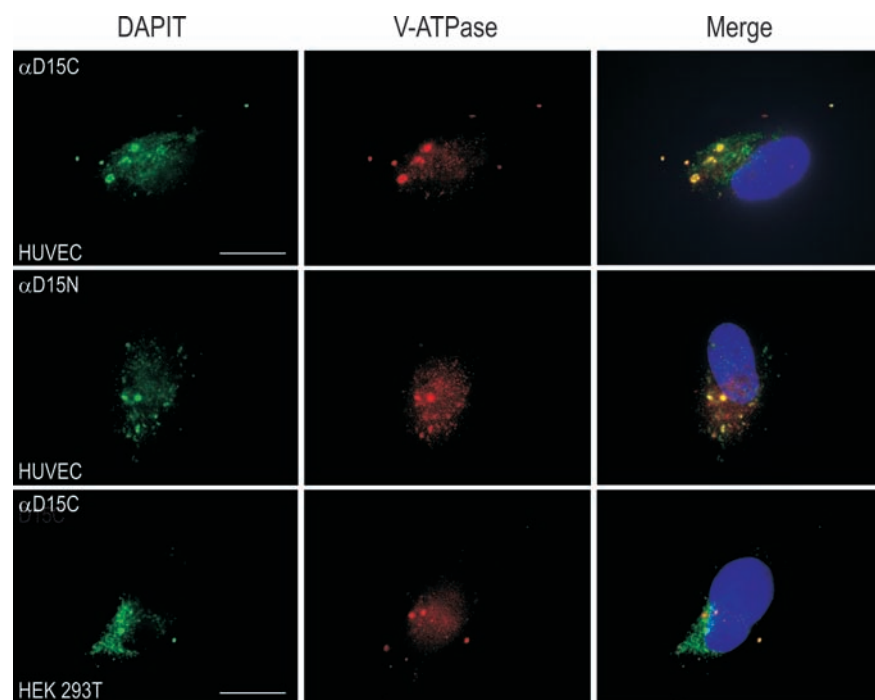


Figure 5. DAPIT locates into vacuoles containing V-ATPase in HUVEC and HEK 293T cells. Nuclei-staining with DAPI. Scale bars: 25  $\mu$ m.



various disease processes.<sup>12</sup> We ascertained by microscopy that DAPIT localizes to lysosomes, which are acidified by V-ATPase.

Our finding promotes the idea that DAPIT could be a component of V-ATPase complex. Since DAPIT has a predicted transmembrane helical span it presumably participates in the formation of the  $V_0$  subunit of the proton pump. Our N-terminal antibody against DAPIT recognized vacuolar protein in HUVEC cells whereas the carboxyterminal both in HUVEC and HEK 293T cells. This suggests that different cell types may have variation in the structure of V-ATPase. Whether DAPIT is a mere structural component or it has a regulatory function in V-ATPases remains to be shown.

DAPIT amino acid sequence is conserved from the yeast to mammalia<sup>1,3</sup> implying its fundamental significance for organisms. In histological studies, we showed the DAPIT expression in several healthy rat and human tissues. In all studied tissues DAPIT showed smeary and granular-type expression, which was most intensive in tissues known to contain copious mitochondria, such as cardiac and skeletal muscle cells and hepatocytes, and epithelial cells related to active transport of nutrients and ions.

The expression of DAPIT requires further studies in insulin-sensitive tissues of diabetic rat and mouse. Previously we showed that DAPIT mRNA was down-regulated in the myocardium and skeletal muscle in early type I diabetes.<sup>1</sup> However, the protein level was regulated differentially. DAPIT was up-regulated in insulin-sensitive rat tissues, except in liver. However, no change in DAPIT protein expression was seen in mouse calf muscle complex after 1-5 weeks of streptozotocin-induced diabetes. This seemingly contradicting data may be due to sample heterogeneity since these muscles have different compositions highly oxidative type I and type II fibers containing plenty of mitochondria and glycolytic type IIb fibers that contain only a low amount of mito-

chondria. Differential expression of mRNA and protein in rat suggests that DAPIT is post-transcriptionally regulated. Since DAPIT is a component of mitochondrial oxidative machinery, one might expect to observe down-regulation of DAPIT in diabetes that is accompanied with impaired mitochondrial function and number in myocardium and skeletal muscles.<sup>13</sup> The significance of the differential DAPIT expression in diabetic tissues and how DAPIT may be implicated in the etiology of diabetes remains to be shown.

In the present study, we characterized custom-made antibodies against DAPIT. In addition to DAPIT protein, the antibody specific for the carboxyterminus of DAPIT recognizes also a larger, unrecognized protein in rat skeletal muscle. Furthermore, we confirmed the presence of DAPIT in mitochondria and showed that it is also located in lysosomes and in other acidic vacuoles. We propose that in addition to being a component of mitochondrial ATP synthase DAPIT is also a subunit of V-ATPase. The significance and possible functions of DAPIT remain to be elucidated.

## References

1. Päivärinne H, Kainulainen H. DAPIT, a novel protein down-regulated in insulin-sensitive tissues in streptozotocin-induced diabetes. *Acta Diabetol* 2001;38: 83-6.
2. Chen R, Runswick MJ, Carroll J, Fearnley IM, Walker JE. Association of two proteolipids of unknown function with ATP synthase from bovine heart mitochondria. *FEBS Lett* 2007;581:3145-8.
3. Meyer B, Wittig I, Trifilieff E, Karas M, Schagger H. Identification of two proteins associated with mammalian ATP synthase. *Mol Cell Proteomics* 2007;6:1690-9.
4. Ohsakaya S, Fujikawa M, Hisabori T, Yoshida M. Knockdown of DAPIT (diabetes-associated protein in insulin-sensitive tissue) results in loss of ATP synthase in mitochondria. *J Biol Chem* 2011;286: 20292-6.
5. Imamura H, Nakano M, Noji H, Muneyuki E, Ohkuma S, Yoshida M, et al. Evidence for rotation of V1-ATPase. *Proc Natl Acad Sci USA* 2003;100:2312-5.
6. Hirata T, Iwamoto-Kihara A, Sun-Wada GH, Okajima T, Wada Y, Futai M. Subunit rotation of vacuolar-type proton pumping ATPase: Relative rotation of the G and C subunits. *J Biol Chem* 2003;278:23714-9.
7. Hulmi JJ, Silvennoinen M, Lehti M, Kivelä R, Kainulainen H. Altered REDD1, myostatin and Akt/mTOR/FoxO/MAPK signaling in streptozotocin-induced diabetic muscle atrophy. *Am J Physiol Endocrinol Metab* 2012;302:E307-15.
8. Hughes SM, Cho M, Karsch-Mizrachi I, Travis M, Silberstein L, Leinwand LA, et al. Three slow myosin heavy chains sequentially expressed in developing mammalian skeletal muscle. *Dev Biol* 1993;158:183-99.
9. Schagger H, Aquila H, Von Jagow G. Coomassie blue-sodium dodecyl sulfate-polyacrylamide gel electrophoresis for direct visualization of polypeptides during electrophoresis. *Anal Biochem* 1988;173: 201-5.
10. Laemmli UK. Cleavage of structural proteins during the assembly of the head of bacteriophage T4. *Nature* 1970;227:680-5.
11. Jefferies KC, Cipriano DJ, Forgac M. Function, structure and regulation of the vacuolar (H<sup>+</sup>)-ATPases. *Arch Biochem Biophys* 2008;476:33-42.
12. Hinton A, Bond S, Forgac M. V-ATPase functions in normal and disease processes. *Pflugers Arch* 2009;457:589-98.
13. Patti ME, Corvera S. The role of mitochondria in the pathogenesis of type 2 diabetes. *Endocr Rev* 2010;31:364-95.